Sulfate Ion Diffusion Assessment of Blended Cement Concrete with Fly Ash and Limestone Powder

Ali H. Shalan, M.ASCE[1]; and Mohamed M. El-Gohary[2]

Abstract: Limited data are available on the measurement of sulfate diffusivity in blended cement-based materials. An experimental study of the diffusion of magnesium sulfate ions in blended cement concrete was performed using different blending materials: fly ash, and lime powder. Different values of cement blending ratio, water–binder ratio, and binder content were studied. Compressive strength loss and weight loss tests were performed to assess the sulfate resistance of the studied mixes. The diffused amount of magnesium sulfate ions was measured using a titration test at different depths from the concrete surface and at different ages up to 12 months of sulfate attack. Fick's second law of nonlinear diffusion was solved using the error function method to develop a simplified model to estimate the sulfate ions diffusion coefficient with different blending materials. These simplified models are a function of the cement blending ratio, water–binder ratio, and binder content. The initial compressive strength decreased by 15.8% and 31.6% for blended cement concretes with 40% fly ash and lime powder, respectively. The weight loss of concrete decreased by 16% at a 40% fly ash blending ratio, whereas it increased by 33.3% at a 40% lime powder blending ratio. The blended cement with fly ash and lime powder had a greatly reduced concrete diffusion coefficient, by 38% and 14% for fly ash and limestone powder, respectively, despite its lower initial compressive strength. The proposed model performed well in simulating sulfate ion ingress in concrete compared with previously published models; it had the best mean value (0.958) and the lowest standard deviation (0.122). **DOI: 10.1061/JSDCCC.SCENG-1610.**

Author keywords: Sulfate ions; Diffusion; Titration test; Fick's law; Blended cement; Fly ash; Lime.

Introduction

Sulfate attack on concrete is a complex process that can lead to the deterioration of structures. The resistance of concrete to sulfate attack is crucial in ensuring the longevity and durability of concrete structures (Diab et al. 2019). However, determining the appropriate value of the sulfate diffusion coefficient can be challenging due to various experimental conditions and limited reported data (Marchand et al. 1999). Different researchers have used different diffusion coefficients, ranging from 0.75×10^{-12} to 9.0×10^{-12} m^2/s, in their sulfate attack models, often without specific justification. The reactions between penetrating sulfates and cement paste can significantly affect the diffusion process. As a result, the effective diffusivity, which represents the actual diffusion behavior in the presence of a sulfate attack, may differ from the intrinsic diffusivity (Chatterji 1995). To estimate the intrinsic diffusivity, some researchers have used the error function solution of Fick's law and concentration experimental data to determine an "effective diffusivity" parameter, denoted D_{eff} (Locoge et al. 1992). This measured value provides an estimation of the intrinsic diffusivity by considering the diffusion-reaction equation. Further research and experimentation are needed to better understand the complexities of sulfate attack on concrete and to accurately determine the appropriate diffusion coefficient for different scenarios (Tixier and Mobasher 2003a).

Blended cements, which incorporate supplementary cementitious materials (SCMs) in addition to clinker and gypsum, have become more prevalent in recent years compared with ordinary portland cement (OPC). These SCMs can include fine limestone, granulated ground blast furnace slag, fly ash (FA), calcined clay, natural pozzolans, and silica fume (Li et al. 2022). The increasing focus on climate change and sustainability in the concrete industry also has driven the wider adoption of SCMs. One of the main advantages of using SCMs is their ability to reduce the clinker factor in cement production. Clinker, which is the main component of OPC, requires a significant amount of energy and releases a substantial amount of carbon dioxide during its production. By replacing a portion of clinker with SCMs, the carbon footprint of cement manufacture can be reduced, contributing to a more sustainable concrete industry (Shalan and El-Gohary 2022; Zunino and Scrivener 2019). In addition to their environmental benefits, SCMs can enhance the sulfate resistance of Portland cement-based materials. Physically, most SCMs can refine the pore structure of the material, making it more compact and less permeable to sulfate ions. This refinement of the pore structure can slow the transportation of sulfate ions, thereby improving the resistance of the cementitious material to sulfate attack (Gao et al. 2022; Huang et al. 2023; Zunino and Scrivener 2022). By incorporating SCMs into blended types of cement, it is possible to achieve a more sustainable and sulfate-resistant concrete that meets both environmental and durability requirements. The specific choice and proportion of SCMs may vary depending on the desired properties and local conditions. However, it is essential to consider the potential effects of SCMs on other aspects of concrete performance, such as strength development, setting time, and workability, to ensure that the desired performance targets are met.

[1]Lecturer, Dept. of Construction and Building Engineering, Higher Institute of Engineering and Technology, Elbeheira 22699, Egypt (corresponding author). Email: dr_alishalan@yahoo.com

[2]Lecturer, Dept. of Construction and Building Engineering, Higher Institute of Engineering and Technology, Elbeheira 22699, Egypt. Email: Mohamedelgohary14@hotmail.com

Note. This manuscript was submitted on March 13, 2024; approved on June 26, 2024; published online on November 26, 2024. Discussion period open until April 26, 2025; separate discussions must be submitted for individual papers. This paper is part of the ***Journal of Structural Design and Construction Practice***, © ASCE, ISSN 2996-5136.

In previous research, various models have been developed to study the transport of ions and the diffusion process in concrete, specifically regarding sulfates. Two main types of models have been used: those based on Fick's second law, and those utilizing the finite-element method (Chen et al. 2020b; Li et al. 2023). Any model addressing sulfate attack should consider the chemical reactions between sulfate ions and the concrete compositions. One developed model takes into account the effective diffusion coefficient, mechanical properties, capillary porosity, and cement composition (specifically, the content of reactive calcium aluminate) to assess the sulfate resistance of concrete (Tixier 2000; Tixier and and Mobasher 2003a, b). Regular-strength concrete and mortar typically exhibit sulfate diffusivities in the range 2.0×10^{-12} to 20×10^{-12} m^2/s. Another expression for cementitious materials was introduced by Samson et al. (2003). This model was developed by Samson et al. (2005). However, the calculated diffusion coefficient using this relationship did not consider the initial capillary porosity, which is a crucial factor to consider (Chen et al. 2018). To address this limitation, a hyperbolic function similar to the analysis of moisture diffusivity has been adopted, yielding comparable trends to the relationship proposed by Samson and Marchand (2007). These models provide valuable insights into evaluating and predicting the diffusion behavior of sulfate ions in concrete. However, the selection of an appropriate model should consider various factors, including the specific objectives of the study, the available data, and the accuracy required for the given application. It also is important to refine and improve these models continually based on new experimental data and insights gained from further research.

The diffusion coefficient equations obtained using previously published models are presented in this section.

An expression for cementitious materials was proposed by Samson et al. (2003)

$$D_{\text{eff}} = e^{(4.3\Phi_{\text{cap}}/V_p)} e^{-(4.3\Phi_{\text{cap}}/V_p)} D_0 \tag{1}$$

where D_0 is a reference value; V_p = paste volume of material (m^3/m^3 of material); and Φ_{cap} = total capillary porosity.

Another diffusion coefficient relationship was developed by Samson et al. (2005)

$$D_{\text{eff}} = D_0 \frac{e^{(4.3/V_p)(\Phi_{\text{ini}} + \sum_{i=1}^{m}(V_i^{\text{ini}} - V_i))}}{e^{(4.3\Phi_{\text{cap}}/V_p)}} \tag{2}$$

where φ_i and φ_{cap} = initial and total capillary porosity of concrete, respectively.

A hyperbolic function similar to the analysis of moisture diffusivity was proposed by Samson and Marchand (2007):

$$D_{\text{eff}} = D_0 + (D_1 - D_0) \cdot f(\beta_D, \varphi_{\text{cap}}) \tag{3}$$

$$f(\beta_D, \varphi_{\text{cap}}) = \frac{e^{-\beta_D} \cdot \zeta}{1 + (e^{-\beta_D} - 1)\zeta}, \quad \text{where } \zeta = \frac{\varphi_{\text{cap}}}{\varphi_i} \tag{4}$$

According to the Mobasher and Tixier model, sulfate ion diffusivity can be estimated based on the chloride ions diffusivity (Tixier 2000; Tixier and and Mobasher 2003a, b)

$$D_{\text{eff}} = D_{\text{Cl}} \left(\frac{D_{f\text{SO}_4}}{D_{f\text{Cl}}} \right)^{2/b} \tag{5}$$

From this expression, it is possible to calculate sulfate diffusivity D_{eff} if chloride diffusivity D_{Cl} is in the range 1.0×10^{-12} to 10×10^{-12} m^2/s and using a value of $D_{f\text{Cl}}$ at 25°C of 2.03×10^{-9} m^2/s and a value of $D_{f\text{SO}_4}$ of 1.0×10^{-9} m^2/s. The numerical model STADIUM follows (Bonakdar et al. 2012; Galíndez and Molinero 2010):

$$D_{\text{eff}} = D_0[0.01 + 0.07\emptyset^2 + 1.8H(\emptyset - \emptyset_c)(\emptyset - \emptyset_c)^2] \tag{6}$$

The GEM equation proposed by Oh and Jang (2004) for diffusion coefficient calculation can be derived in terms of the normalized diffusivities as follows:

$$D_{\text{eff}} = D_0 \left(m_\emptyset + \sqrt{m_\emptyset^2 + \frac{\emptyset_c}{1 - \emptyset_c} \left(\frac{D_s}{D_0} \right)^{1/n}} \right)^n \tag{7}$$

where D_s/D_0 = normalized diffusivity of solid phase, which denotes the diffusivity when capillary porosity equals zero, and depends on the complexity of the structure of the hydrated solid matrix. Realistic values for n and D_s/D_0 obtained from test data are $n = 2.7$ and $D_s/D_0 = 2.0 \times 10^{-4}$ for portland cement pastes.

In recent years, the exploration of sulfate ion diffusion in concrete has gained considerable momentum, with a focus on utilizing advanced chemomechanical modeling and finite-element modeling techniques (Chen et al. 2020a; Li et al. 2023). A significant body of research has emerged over the last half-decade investigating the intricate chemical reactions between sulfate ions and hydration products within concrete matrices to accurately replicate the diffusion phenomena (Wu et al. 2023). This surge in studies underscores the growing recognition of the critical impact that sulfate ions can have on concrete durability and performance (Diab et al. 2019). In particular, finite-element modeling has garnered attention as a cutting-edge methodology for simulating and predicting sulfate ion diffusion processes in concrete structures (Jin et al. 2024). Leveraging the power of computer modeling and data-driven models, these innovative techniques offer enhanced precision and efficiency in simulating the complex interplay between sulfate ions and concrete constituents, paving the way for more-sophisticated and -robust analytical frameworks in the realm of concrete technology.

This study investigated the chemical and mechanical changes that occur when concrete is subjected to an external sulfate attack. The research compared the behavior of two types of cement: control (portland cement), and blended cement [composed of Class F fly ash and limestone powder (LS)]. To assess the ionic diffusion, concrete samples were prepared, and concentration profiles were measured for major elements. The diffusion data were collected in one dimension and compared with predicted values obtained from diffusion equations. The accuracy of the proposed model was evaluated based on this comparison. The diffusion and chemical changes were analyzed using the titration test method specified in ASTM E738-11 (ASTM 2007). This analysis allowed for the measurement of diffusion and chemical alterations caused by the sulfate attack. The study considered various factors in the experimental design, including different blending ratios, water–binder ratios, binder content, and types of blending materials. Examining these variables provided insight into the behavior of different cement mixtures under sulfate attack conditions. Furthermore, the results obtained from the proposed model were compared with other published models that have been discussed in the literature. This comparative analysis provided a comprehensive evaluation of the proposed modeling framework and its effectiveness in predicting the behavior of blended cement types under sulfate attack conditions. Overall, the findings of this research are expected to contribute to the design of concrete materials, particularly in terms of selecting appropriate blended cement types to enhance resistance against sulfate attack.

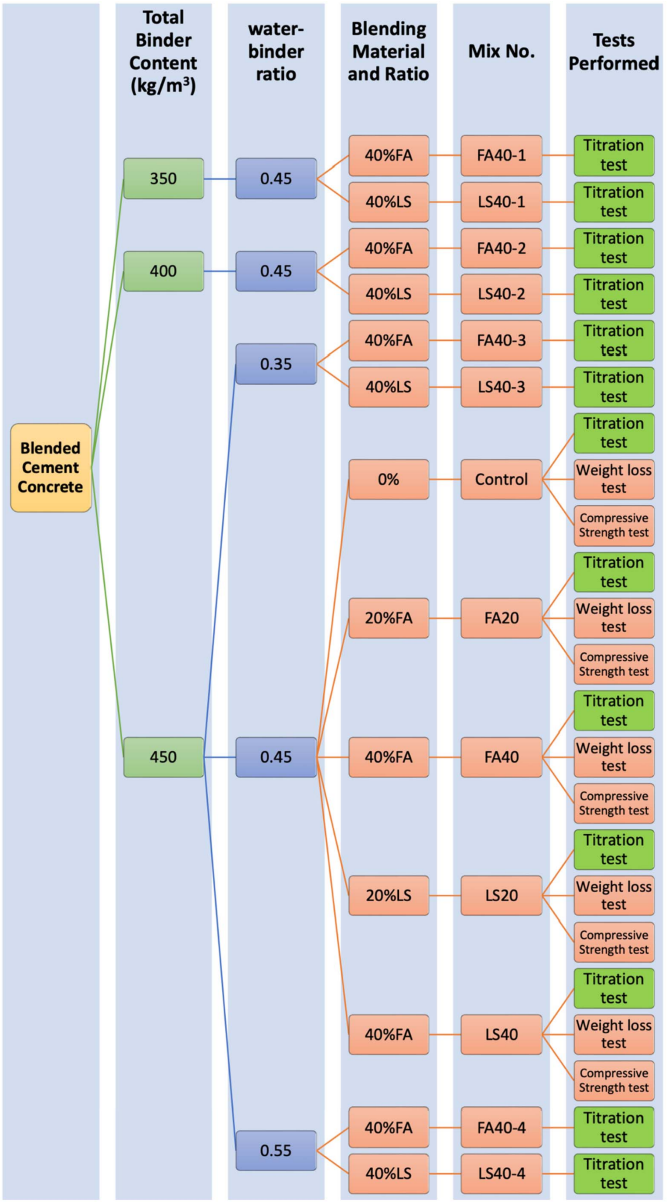

Fig. 1. Flowchart of the research experimental program.

Materials and Methods

The experimental program performed in this research is displayed Fig. 1, which presents a flowchart of program details. Ordinary portland cement according to ASTM C150-07 (ASTM 2009) was used in this research work. Two replacement materials were used in this study: fly ash, and ground limestone powder. The chemical and physical properties of the cement, fly ash, and limestone are presented in Table 1 according to ASTM C618 (ASTM 2015) limits. The used sand was natural siliceous sand with a fineness modulus of 2.70. Crushed pink limestone (9.75-mm nominal maximum size) was used as coarse aggregate. These aggregates fulfilled the requirements of ASTM C115-96 (ASTM 1996). Superplasticizer (SP) Type F in accordance with ASTM C494/C494M-11 (ASTM 2012) was used in the concrete mixes to achieve a constant slump for concrete of 12 cm $\pm$ 2 cm.

Thirteen concrete mixes were used to determine the magnesium sulfate ion concentration that diffuses in concrete for up to 12 months. The proportions of the control mix were calculated according to the ACI 211.1-91 (ACI 1991) mix proportioning method to resist magnesium sulfate attack. The cement content was modified in the other mixes using different blending ratios of fly ash and ground limestone: 20% and 40% at a water–binder ratio of 0.45 and 450 kg/m^3 binder content. The mix proportions of 1 m^3 of concrete mixes used in this study are listed in Table 2. The chemical composition of the blended binder mixtures are presented in Table 3. At a 40% blending ratio, the water–binder ratio was changed to 0.35 and 0.55, and the binder content was varied from 450 kg/m^3 to 350 and 400 kg/m^3.

Concrete specimens were immersed in 5.0% magnesium sulfate solution (70.42 mol/m^3) after 7 days of curing in water. The sulfate solution was replaced every 4 weeks to keep a constant pH value. A chemical analysis of titration test according to ASTM E738-11 was used to measure the sulfate ion content at different depths of concrete specimens. Samples at different depths (1.0, 4.0, 7.0, 10, 15, and 20 mm) in the specimens were extracted by drilling. To study the diffusion rate of sulfate ions in concrete over time, the sulfate ion content was measured at 4, 8, and 12 months of exposure age. This test was carried out using 150 × 150 × 150-mm cubes, which were sealed on five faces to produce a linear diffusion for ions. Three concrete 150 × 150 × 150-mm cubes were tested for compressive strength at an age of 28 days according to BS EN 12390-1 (BSI 2009). The compressive strength loss percentage due to magnesium sulfate attack was measured based on the method described in ASTM C267-01 (ASTM 2005). Concrete cubes were immersed in a 5.0% magnesium sulfate solution for 4, 8, and 12 months. Following 28 days of water curing, the weight loss percentage of the concrete was tested after 4, 8, and 12 months based on the method described in ASTM C267-01. Sets of three cubes (100 × 100 × 100 mm) from each mixture were submerged in 5% magnesium sulfate solution.

When a concrete specimen is subjected to sulfate attack under the ambient ion concentration C_0, the ion transfer processes are described as one-dimensional (1-D) nonsteady diffusion (Fig. 2). The molar concentration of the sulfate ions diffuses from the sulfate solution to the interior of the specimen. Therefore, the diffusion equation can be expressed by Fick's second law as (Crank 1979)

$$\frac{\partial C}{\partial t} = D_{\text{eff}} \frac{\partial^2 C}{\partial x^2} \tag{8}$$

where $C = c(x, t)$ = sulfate ion concentration; x and t = section position and time, respectively; and D_{eff} = effective diffusion

Table 1. Chemical and physical properties of cement, fly ash, and ground limestone

Material	Chemical composition (%)							LOI (%)	Specific gravity	Fineness, percentage retained on #325 sieve
	CaO	SiO_2	SO_3	Al_2O_3	Fe_2O_3	MgO	$SiO_2 + Al_2O_3 + Fe_2O_3$			
OPC	62.6	19.90	2.90	5.10	3.60	1.50	—	1.20	3.15	31
FA	3.23	49.90	0.88	24.0	14.40	0.98	88	2.50	2.20	22
LS	86.94	6.50	0.42	0.11	0.19	1.23	—	42.5	2.72	12
ASTM C618 limit	—	—	<5.0	—	—	—	>70	<6.0	—	<34

Note: LOI = loss on ignition.

Table 2. Mix proportions for 1 m^3 of blended cement concretes with FA and LS

Mix no.	Total binder (kg)	w/b	Cement (kg)	FA (kg)	LS (kg)	Water (kg)	Crushed stone (kg)	Sand (kg)	SP (kg)
Control	450	0.45	450	0	0	202.5	840	785	6.75
FA20	450	0.45	360	90	0	202.5	840	769	7.09
FA40	450	0.45	270	180	0	202.5	840	753	7.43
FA40-1	350	0.45	210	140	0	157.5	0	1,828	5.78
FA40-2	400	0.45	240	160	0	180	0	1,722	6.60
FA40-3	450	0.35	270	180	0	157.5	0	1,729	9.90
FA40-4	450	0.55	270	180	0	247.5	0	1,504	4.95
LS20	450	0.45	360	0	90	202.5	840	772	7.43
LS40	450	0.45	270	0	180	202.5	840	758	8.10
LS40-1	350	0.45	210	0	140	157.5	0	1,832	6.30
LS40-2	400	0.45	240	0	160	180	0	1,727	7.20
LS40-3	450	0.35	270	0	180	157.5	0	1,739	8.10
LS40-4	450	0.55	270	0	180	247.5	0	1,504	8.10

Table 3. Chemical compositions of blended binder mixtures with FA and LS

Mix no.	Binder blending ratio (%)			Blended binder chemical composition						Blaine surface area (m^2/kg)
	Cement	FA	LS	CaO (C) (%)	SiO_2 (S) (%)	Al_2O_3 (%)	C/S	C + S (%)	C_3A (%)	
Control	100	0	0	62.60	19.90	5.10	3.15	82.50	10.92	340
FA20	80	20	0	50.18	28.38	9.70	1.77	78.56	8.74	350
FA40	60	40	0	37.76	36.86	14.30	1.02	74.62	6.55	360
FA40-1	60	40	0	37.76	36.86	14.30	1.02	74.62	6.55	360
FA40-2	60	40	0	37.76	36.86	14.30	1.02	74.62	6.55	360
FA40-3	60	40	0	37.76	36.86	14.30	1.02	74.62	6.55	360
FA40-4	60	40	0	37.76	36.86	14.30	1.02	74.62	6.55	360
LS20	80	0	20	67.47	17.22	4.10	3.92	84.69	8.74	370
LS40	60	0	40	72.34	14.54	3.10	4.97	86.88	6.55	400
LS40-1	60	0	40	72.34	14.54	3.10	4.97	86.88	6.55	400
LS40-2	60	0	40	72.34	14.54	3.10	4.97	86.88	6.55	400
LS40-3	60	0	40	72.34	14.54	3.10	4.97	86.88	6.55	400
LS40-4	60	0	40	72.34	14.54	3.10	4.97	86.88	6.55	400

coefficient of sulfate ions in concrete. Due to the chemical reactions between sulfate ions and cement, the sulfate concentration can be depleted (decreased). According to Crank, due to the effect of sulfate depletion, the second Fick's law can be modified as (Crank 1979)

$$\frac{\partial C}{\partial t} = D_{\text{eff}} \frac{\partial^2 C}{\partial x^2} - \frac{\partial C_d}{\partial t} \tag{9}$$

where C_d = depleted sulfate ion concentration due to chemical reactions. Depending on the dynamical equation of the chemical reaction, the rate of depletion can be estimated using the following formula (Gospodinov et al. 1996):

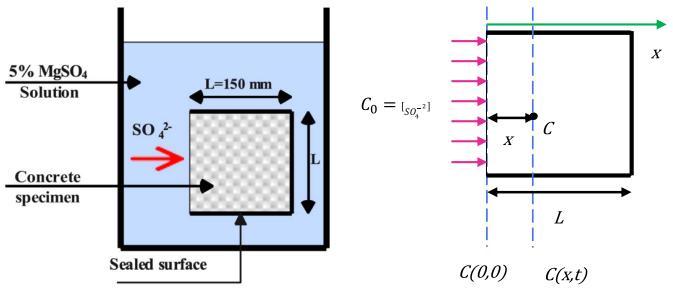

Fig. 2. Diffusion of sulfate ions in concrete specimens.

$$\frac{\partial C_d}{\partial t} = kC^0_{C_3A} f(c,t) Ce^{-(1/3)kct} \tag{10}$$

where k = reaction rate between sulfate ion and cement hydrated products (0.00015 $m^3/mol/day$); $C^0_{C_3A}$ = initial C_3A content in cement; and $f(c,t)$ is determined as (Gospodinov et al. 1996)

$$f(c,t) = 1 - h_\alpha + \frac{1}{2}\beta h_\alpha + \beta h_\alpha e^{-(1/6)kct} \tag{11}$$

where β = initial gypsum content in cement; and h_α = hydration degree of cement related to hydration time, which can be determined approximately as (Gospodinov et al. 1996)

$$h_\alpha = 1 - 0.5[(1+1.67t)^{-0.6} + (1+0.29t)^{-0.48}] \tag{12}$$

The experimental test results were used in Eqs. (10)–(12) with the known value of k (Gospodinov et al. 1999). The value of D_{eff} can be calculated using the error function solution method (Crank and Gupta 1972)

$$C(x,t) + C_d(t) = C_0\left(1 - \text{erf}\frac{x}{2\sqrt{D_{\text{eff}}t}}\right) \tag{13}$$

Table 4. Compressive strength test results and compressive strength loss at different exposure ages compared with 28-day compressive strength

Mix ID	Cube compressive strength (MPa)			Residual cube compressive strength after sulfate attack (MPa)			Compressive strength loss percentage after sulfate attack (%)		
	7 days	28 days	90 days	4 months	8 months	12 months	4 months	8 months	12 months
Control	32.5	46.2	54.5	37.8	34.8	33.2	18.2	24.7	28.2
FA20	30.9	43.3	50	37.8	35.3	33.2	12.6	18.4	23.3
FA40	30.2	38.9	47.2	33.4	31.1	28.9	14.1	20.1	25.6
LS20	24.8	34.8	44.9	27.6	25.2	23.9	20.7	27.6	31.2
LS40	20.7	31.6	40.5	24.0	21.7	20.1	24.2	31.4	36.3

Results

Compressive Strength Loss Test

The results of the compressive strength tests for all mixes in this study (Table 4) revealed a decrease in compressive strength as the volume of replacement materials increased [Fig. 3(a)]. Compared with that of the control mix, the 28-day compressive strength of blended cement concretes decreased by 6%, 15.8%, 24.7%, and 31.6% for the FA20, FA40, LS20, and LS40 mixes, respectively. The significant reductions in compressive strength for LS concrete can be attributed to defects within the mortar, which has a lower density than the stone aggregate, thus leading to a decrease in strength (Wang et al. 2013). The addition of 20% and 40% FA to the concrete mix resulted in compressive strength reductions of 6.2% and 15.8% at 28 days, respectively. However, the compressive strength of FA concrete substantially improved (by approximately 15%) between 28 and 90 days, even though it did not reach the strength of the control mix. This behavior of FA concrete commonly is attributed to the slow reaction of its aluminosilicate particles with free portlandite to produce cementing compounds, i.e., calcium-aluminum-silicate hydrates. At a higher replacement ratio of FA, the fraction of particles acting as filler increases because of the overall reduction in calcium oxide content of the binder (Kurad et al. 2017).

The incorporation of fly ash and cement in blended cement against sulfate attack had a noticeably smaller negative effect than was expected [Fig. 3(b)]. Kou et al. (2011) and Kurad et al. (2017) reported similar findings, in which pozzolans such as fly ash have fewer amaging effects on the strength properties of concrete compared with those in low-strength concrete. This can be attributed to the presence of portlandite (CH) in the attached mortar, which reacts with FA particles at the interface transition zones (ITZs) between the binder matrix and aggregates. This reaction minimizes the negative impact of high-volume FA incorporation on the strength of FA concrete. Additionally, the strength development rate of FA concrete, between the ages of 28 and 90 days was found to accelerate with an increase in the level of replacement. This indicates that the pozzolanic potential of FA concrete increases with a higher percentage of replacement.

Overall, the results of the study showed that the chemical activation of FA had a positive impact on the compressive strength loss of concrete at all exposure ages. In particular, the use of FA in concrete mixes resulted in less compressive strength loss than in the control mixes at 4, 8, and 12 months of exposure. This can be attributed to the increased reactivity of FA when exposed to calcium hydroxide in the presence of sulfate. According to previous research by Qian et al. (2001), sulfates react directly with calcium hydroxide, contributing to the formation of ettringite. This reaction not only strengthens the concrete but also produces a strong alkali solution that helps to dissolve the silica particles in the FA. This dissolution of silica particles further increases the alkalinity around FA particles, resulting in a more effective activation of the FA. This phenomenon has been observed in previous studies by Velandia et al. (2016, 2018) and Hefni et al. (2018), in which the use of sulfates in high-volume FA concretes led to improved strength and durability properties.

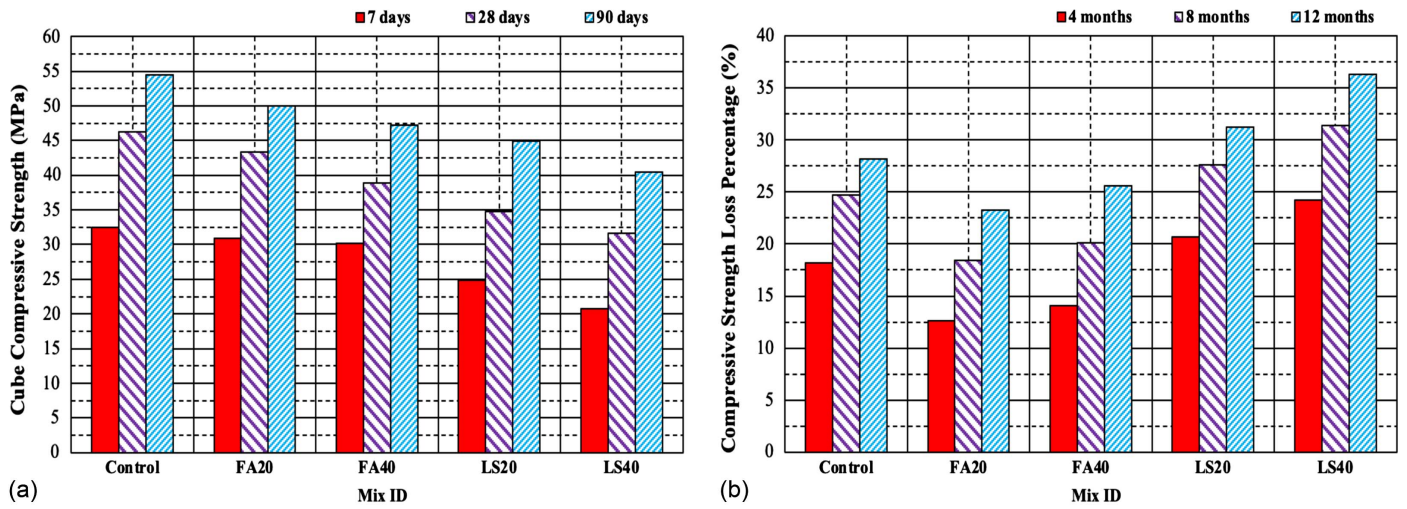

Fig. 3. Properties of blended cement concrete with fly ash and limestone powder: (a) cube compressive strength; and (b) compressive strength loss percentage.

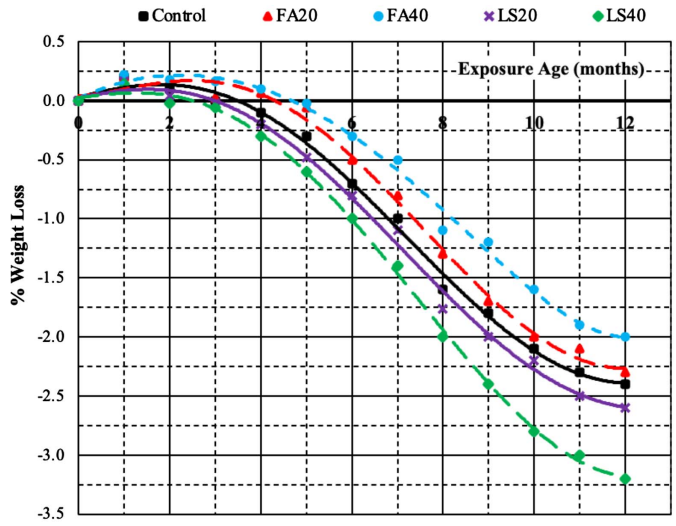

Fig. 4. Relationship between sample weight loss percentage and exposure age for different blended binders with fly ash and limestone powder.

Weight Loss Test

To assess the sulfate attack resistance of concrete mixes, a common metric used is the weight loss due to erosion caused by exposure to a magnesium sulfate solution. This method allows for the evaluation of the material's performance over varying durations, with weight loss after 4, 8, and 12 months of exposure commonly being measured. The findings reported in Fig. 4 demonstrate the significant impact of incorporating high-silica, low-calcium supplementary cementitious materials such as fly ash on the sulfate attack resistance of concrete. As the volume fraction of replacement materials increases, the weight loss of concrete decreases rapidly, signaling the potential benefits of incorporating FA in concrete mixtures. This improvement is attributed to the reduction in the overall production of calcium hydroxide (CH), a key component in the formation of sulfate compounds when FA replaces ordinary portland cement. This is in accordance with previous research studies (Masood et al. 2020), highlighting the potential of FA to mitigate the deleterious effects of sulfate attack on concrete structures. Furthermore, the use of FA also contributes to a decrease in the porosity and sorptivity of concrete, resulting in a slower penetration of sulfate ions into the specimens. This decrease in permeability, combined with the reduced CH production, can significantly enhance the durability and lifespan of concrete structures in sulfate-rich environments.

EDTA Complexometric Titration Test Results

The ethylenediaminetetraacetic acid (EDTA) complexometric titration test was used to determine the relationship between sulfate ion concentration per cubic meter and the depth of the extraction section (Table 5). The titration test was performed on the concrete mixes listed in Table 2. The relationships between the sulfate concentration profile and each studied parameter are presented in Fig. 5, which shows the effect of fly ash and limestone powder replacement ratio on the sulfate ion concentration for concrete with a water–binder ratio of 0.45, and a binder content of 450 kg/m^3 at 12 months of exposure. The sulfate ion concentration decreased as the extraction section depth increased. For example, in the control

Table 5. Experimental results of sulfate ion concentration at different depths at different exposure ages

Mix ID	Age (months)	Sulfate ion concentration profile at different depths (mol/m^3)						
		0	1 mm	4 mm	7 mm	10 mm	15 mm	20 mm
Control	4	70	52.463	37.655	21.540	14.646	0.000	0.000
	8	70	57.880	40.210	24.642	16.394	0.000	0.000
	12	70	65.200	49.650	35.973	26.417	16.000	10.000
FA20	4	70	33.195	22.260	13.668	7.566	0.000	0.000
	8	70	43.537	31.890	22.462	15.196	0.000	0.000
	12	70	59.211	42.220	27.866	20.003	10.898	0.000
FA40	4	70	39.025	22.140	10.779	0.000	0.000	0.000
	8	70	48.535	30.970	18.490	10.354	0.000	0.000
	12	70	56.964	39.440	24.691	15.053	0.000	0.000
FA40-1	4	70	48.018	29.840	16.635	8.197	0.000	0.000
	8	70	59.981	40.500	26.316	16.234	6.579	0.000
	12	70	61.341	46.380	30.970	20.347	9.575	0.000
FA40-2	4	70	38.836	26.960	17.424	10.489	0.000	0.000
	8	70	50.315	37.080	26.798	18.686	9.662	0.000
	12	70	58.215	43.160	27.456	16.545	3.245	0.000
FA40-3	4	70	26.454	17.390	10.365	0.000	0.000	0.000
	8	70	36.153	26.170	18.194	12.121	0.000	0.000
	12	70	37.469	30.250	15.503	8.168	0.000	0.000
FA40-4	4	70	50.148	32.760	19.656	10.584	0.000	0.000
	8	70	56.852	40.290	27.486	18.089	8.199	0.000
	12	70	60.488	46.470	32.318	22.390	11.618	0.000
LS20	4	70	31.325	22.260	14.907	9.267	0.000	0.000
	8	70	45.879	34.400	25.583	18.504	10.109	0.000
	12	70	62.440	44.222	30.900	23.235	14.013	8.144

Table 5. (*Continued*.)

Mix ID	Age (months)	Sulfate ion concentration profile at different depths (mol/m^3)						
		0	1 mm	4 mm	7 mm	10 mm	15 mm	20 mm
LS40	4	70	41.250	24.750	13.010	0.000	0.000	0.000
	8	70	51.545	36.430	22.856	13.574	0.000	0.000
	12	70	58.550	42.460	27.462	17.533	7.816	0.000
LS40-1	4	70	44.325	29.220	17.716	9.754	0.000	0.000
	8	70	66.306	47.090	32.357	21.389	9.924	0.000
	12	70	67.897	49.680	35.153	24.373	12.813	6.267
LS40-2	4	70	40.456	26.310	9.983	0.000	0.000	0.000
	8	70	45.945	38.545	21.741	9.689	0.000	0.000
	12	70	53.115	31.584	24.098	12.239	0.000	0.000
LS40-3	4	70	30.034	21.220	13.929	8.597	0.000	0.000
	8	70	41.105	31.380	23.185	16.598	8.869	0.000
	12	70	41.554	34.940	22.895	8.856	0.000	0.000
LS40-4	4	70	42.560	29.220	18.527	10.799	0.000	0.000
	8	70	53.530	39.270	28.081	19.306	9.653	0.000
	12	70	62.406	49.340	35.718	25.528	14.373	7.594

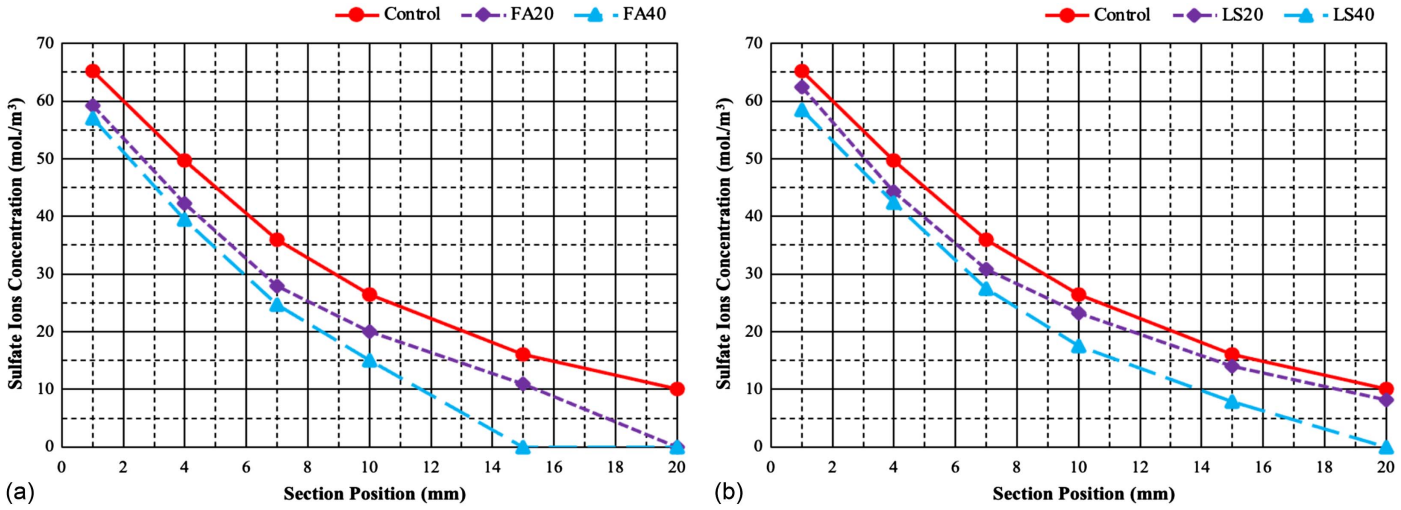

Fig. 5. Relationship between 12-month concentration profile and section position in concrete for different replacement ratios: (a) fly ash; and (b) limestone powder.

mix in Fig. 5(a), the ion concentration decreased by 30% and 64% at 4.0- and 7.0-mm section depths, respectively, compared with sulfate ion concentration at the surface of the specimen, whereas the reduction was 27% and 53% at 4.0- and 7.0-mm section depths, respectively, at a 40% replacement ratio with fly ash compared with that at the surface of the specimen. Fig. 5 provides a visual representation of the connectivity of pores within the microstructure of concrete, giving a rough estimate of the overall porosity of the material. It is evident from experimental results that the concentration of sulfate ions decreased with the increasing levels of cement replacement with fly ash and limestone powder. At 20% and 40% replacement ratios, the sulfate ion concentration decreased by 15% and 21%, respectively. This decrease in sulfate ion concentration can be attributed to the contribution of fly ash and limestone powder to the microstructure development through two distinct mechanisms. Firstly, the pozzolanic reaction of fly ash consumes free calcium hydroxide, resulting in the formation of calcium silicate hydrates. This process is comparatively slower than the hydration process of cement, and thus contributes to the strength of concrete at later ages. Secondly, as a filler material, fly ash effectively fills the spaces between OPC particles, contributing to the strength of concrete at all ages. Similarly, the use of limestone powder also aids in filling the pores in concrete [Fig. 5(b)]. This improved microstructure significantly decreases the permeability of concrete (Dimitriou et al. 2018). For example, at 20% and 40% limestone powder replacement ratios, the sulfate ion concentration decreased by 14%, and 19%, respectively.

In addition, the explicit effect of total binder content is shown in Fig. 6, which presents the effect of total binder content on sulfate ion concentration for concrete with 0.45 water–binder ratio and a 40% replacement ratio. The ion concentration in concrete decreased as the total binder content increased (Fig. 6 and Table 5). This result is logical because the increase in total binder content leads to a decrease in concrete porosity and an increase in cement gel. For example, at a 40% limestone replacement ratio, 12 months of exposure, and 4.0-mm section depth, the ion concentration

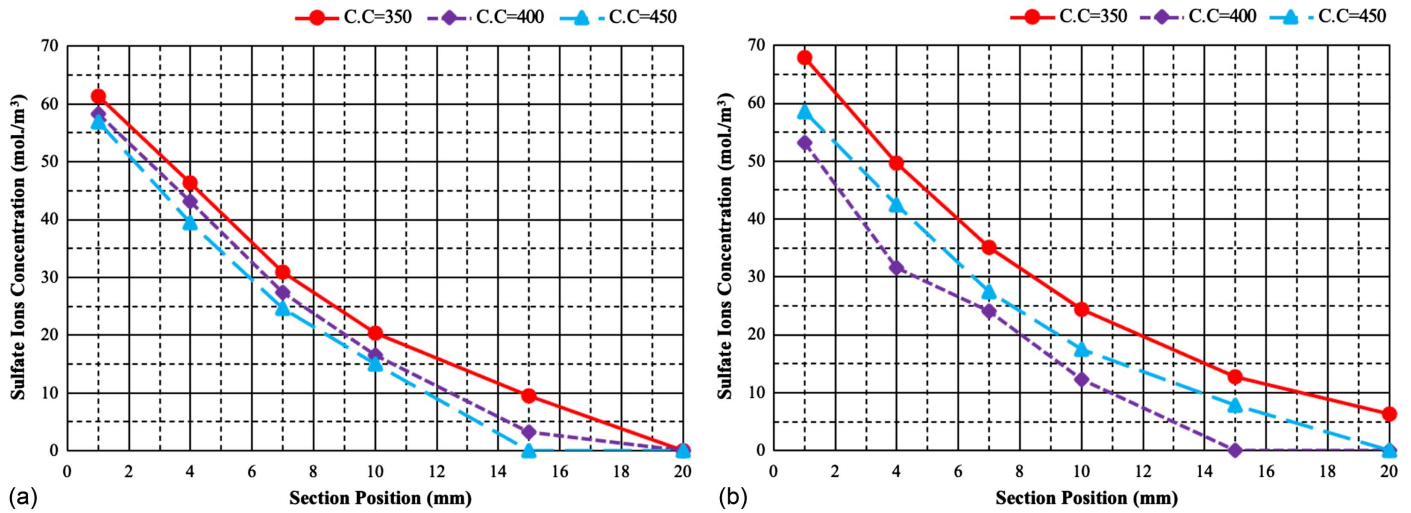

Fig. 6. Relationship between 12-month concentration profile and section position in concrete for different total binder contents: (a) 40% fly ash replacement ratio; and (b) 40% limestone powder replacement ratio.

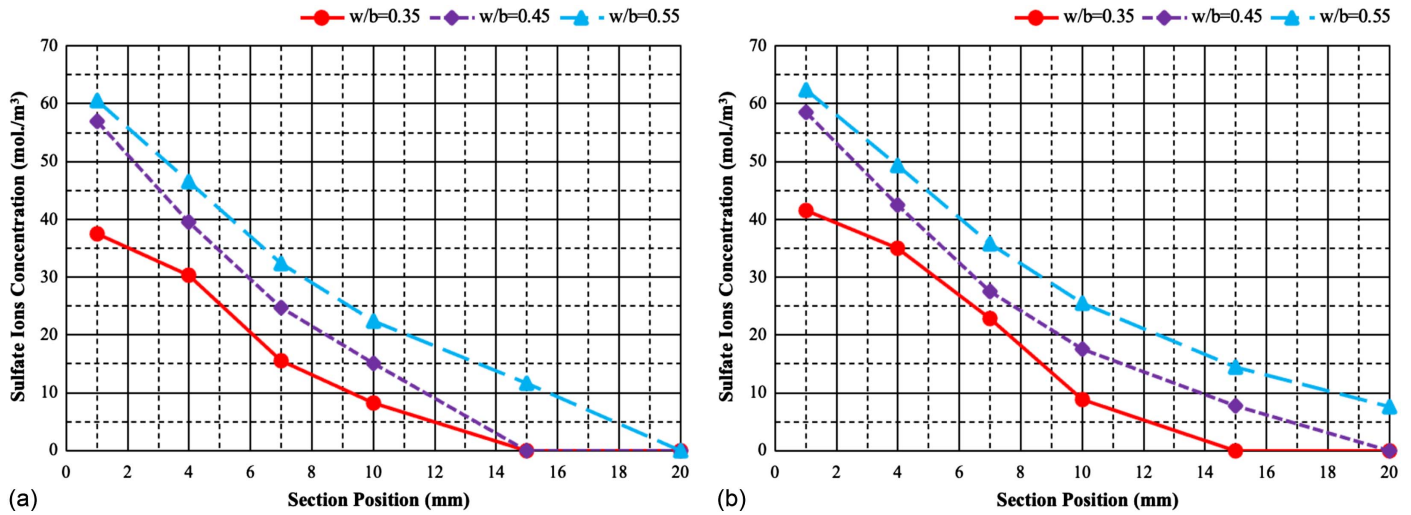

Fig. 7. Relationship between 12-month concentration profile and section position in concrete for different water–binder ratios: (a) 40% fly ash replacement ratio; and (b) 40% limestone powder replacement ratio.

decreased by 13% and 21% as total binder content increased from 350 to 400 and 450 kg/m^3, respectively. The effect of water–binder-ratio on sulfate ion concentration for concrete with 450 kg/m^3 total binder content and a 40% replacement ratio with fly ash and limestone powder. The ion concentration in concrete increased as the water–binder ratio increased for different exposure ages (Table 2 and Fig. 7). This result is logical because the increase in the water–binder ratio leads to an increase in concrete porosity. For example, at 12 months of exposure, a 40% replacement ratio of fly ash, and a 4.0-mm section depth, the ion concentration increased by 30% and 53% as the water–binder-ratio increased from 0.35 to 0.45 and 0.55, respectively. The ion concentration in concrete increased with age at 20% and 40% replacement ratios (Fig. 8). For example, at a 4.0-mm section depth and 40% limestone powder replacement ratio, the ion concentration in concrete was 24.75, 36.43, and 42.46 mol/m^3 at ages of 4, 8 and 12 months, respectively.

Concrete Sulfate Ion Diffusion Coefficient

The sulfate ion diffusion coefficient (D_{eff}) is the measure of Darcian flow through a dried cement-based material under the action of capillary forces; D_{eff} largely is affected by the pore structure of the media, i.e., water-accessible porosity, connectivity, and tortuosity of pores. According to the previous assessment scenario, calculated sulfate diffusion coefficients are presented in Table 6 for a depth of 4.0 mm. These results of the assessment scenario are represented as a relationship between the sulfate ion diffusion coefficient in concrete versus different parameters: cement replacement ratio with fly ash and limestone powder, binder content, water–binder ratio, and exposure to sulfate solution (Fig. 9). This study found significant effects of fly ash and limestone powder on the diffusion coefficient of concrete. The inclusion of these materials led to a drastic decrease in the diffusion coefficient; a 20% replacement of cement with fly ash and limestone powder resulted in a 38% and 14% decrease of the

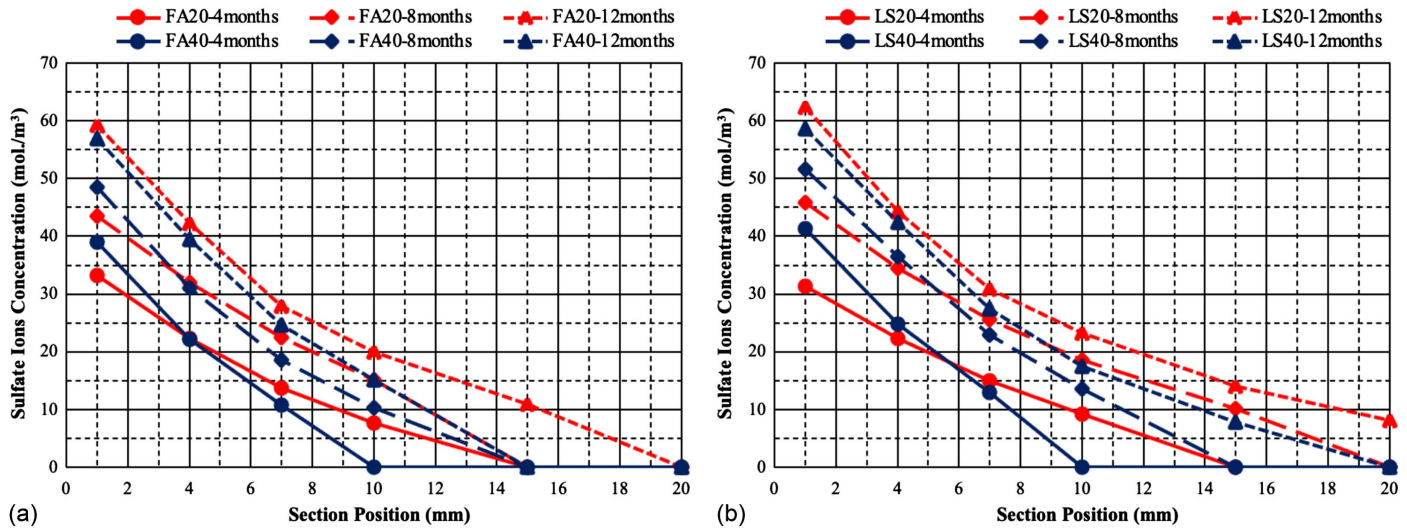

Fig. 8. Relationship between concentration profile and section position in concrete for different ages of exposure: (a) different fly ash replacement ratios; and (b) different limestone powder replacement ratios.

diffusion coefficient, respectively [Fig. 9(a)]. This can be attributed to the highly dense three-dimensional aluminosilicate gel produced as the reaction product in alkali-activated FA, which is denser than the calcium silicate gel produced in traditional cement binders (Provis and van Deventer 2009).

The longer the immersion time of the concrete, the higher was the ion concentration at the concrete surface, resulting in an increase in ion concentration distribution within the concrete because of the established concentration gradient. Fig. 9(b) shows the sulfate ion diffusion coefficient in concrete at exposure ages of 4, 8, and 12 months for concrete with different C_3A contents and water–binder ratios of 0.40, 0.50 and 0.60. The diffusion coefficient decreased with age. However, as the exposure age of the concrete increased, the degree of reaction between sulfate ions and chemical compositions in concrete also increased. As a consequence, these reaction products filled the concrete, reducing internal pores, blocking channels for ion diffusion, and improving overall concrete diffusivity. Consequently, over time, the rate of ion concentration growth within the concrete tended to decrease.

Table 6. Sulfate ion diffusion coefficient at different ages at depth of 4.0 mm

	Sulfate ion diffusion coefficient at different exposure ages (10^{-12} m^2/s)		
Mix ID	4 months	8 months	12 months
Control	4.750	4.176	4.000
FA20	2.934	2.579	2.470
FA40	2.310	2.031	1.946
FA40-1	3.819	3.357	3.216
FA40-2	2.599	2.285	2.189
FA40-3	1.797	1.580	1.513
FA40-4	2.824	2.482	2.378
LS20	4.110	3.613	3.461
LS40	3.654	3.212	3.077
LS40-1	6.108	5.369	5.143
LS40-2	5.344	4.698	4.500
LS40-3	3.695	3.248	3.111
LS40-4	5.806	5.104	4.889

Nevertheless, the dominant force driving ion diffusion remains the difference in concentration gradient between the internal and external solution environments (Wang et al. 2021). For example, in the FA40-1 mix, the diffusion coefficient decreased by 12% and 16% as the age increased from 4 months to 8 and 12 months, respectively. In addition, the explicit effect of binder content is shown in Fig. 9(c), which presents the effect of binder content on sulfate ions diffusion coefficient in concrete with a 0.45 water–binder ratio and 40% replacement ratio with fly ash and limestone powder. The sulfate ions diffusion coefficient in concrete decreased with exposure age as the binder content increased. For example, in the FA40 mix at 12 months of exposure, the diffusion coefficient decreased by 13% and 22% as the binder content increased from 350 to 400 and 450 kg/m^3, respectively.

The positive effect of water–binder-ratio reduction is clear from Fig. 9(d). The sulfate ion diffusion coefficient in concrete with a 450 kg/m^3 total binder content and 40% replacement ratio with fly ash and limestone powder increased with age as the water–binder ratio increased. Furthermore, the distribution of ions in concrete varies based on the capillary porosity, which determines the diffusion coefficient, and its relationship with factors such as water–binder ratio, degree of hydration, and distance from the aggregate surface (Liu et al. 2014). In concrete with a lower water–binder ratio, the pores become smaller after hydration, resulting in higher structural compactness and increased tortuosity (Liu et al. 2014). Consequently, concrete structures with a lower water–cement ratio allow less infiltration of free sulfate ions than do those with a higher ratio, resulting in lower ion concentration in the pore liquid. For example, in the FA40 mix with 12 months of exposure, the diffusion coefficient increased by 29% and 57% as the water–binder ratio increased from 0.35 to 0.45 and 0.55, respectively, whereas the sulfate diffusion coefficient increased by 25% and 53% as the water–binder-ratio increased from 0.35 to 0.45 and 0.55, respectively, in LS40 at 12 months of exposure. Research regarding the factors influencing the diffusion behavior of sulfate ions suggests two crucial parameters in Fick's second law of diffusion: the sulfate ion diffusion coefficient (D_{eff}) (Medeiros and Helene 2009; Shafikhani and Chidiac 2020; Zhang et al. 2018), and the surface sulfate ion concentration (C_0) (Cai et al. 2020, 2021).

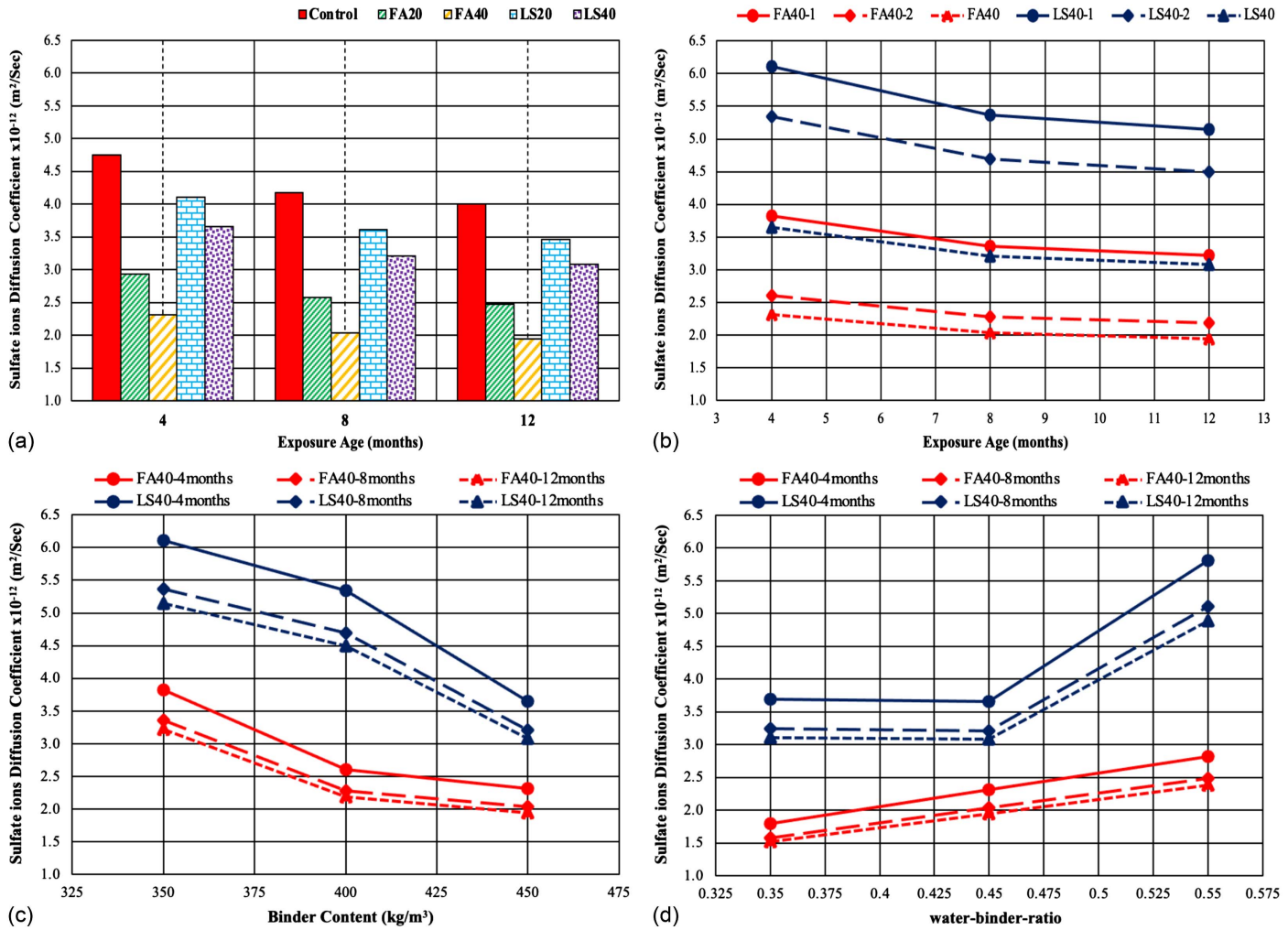

Fig. 9. Relationship between sulfate ions diffusion coefficient of concrete and different (a) fly ash and limestone powder replacement ratios; (b) exposure ages; (c) binder contents; and (d) water–binder ratios.

Establishing the Proposed Model for Concrete Sulfate Ion Diffusion Coefficient Assessment

Because of the absence of a simple equation for calculating the sulfate diffusion coefficient for blended cement concrete depending directly on the main concrete composition, the values of the diffusion coefficient in Table 6 were used to obtain the values of D_{eff} by regression analysis. The equation takes into account the chemical composition of the binder: total calcite and silicate content (C + S), water–binder-ratio (w/b), age (t), and binder content (b). The following model is proposed:

$$D_{\text{eff}} = \frac{\left(\frac{w}{b}\right)(-0.537 \ln t + 6.2077) D_1}{b} \times 10^{-9} \qquad (14)$$

where D_1 can be calculated as follows:

$$D_1 = 1.4137 - 0.1264(\text{C} + \text{S}) - 0.0062(\text{C} + \text{S})^2 \qquad (15)$$

where D_{eff} = effective sulfate ion diffusion coefficient in concrete (m^2/S); t = exposure age of specimen (days); b = cement content (kg/m^3); and (C + S) = total calcite and silicate percentage. Eqs. (14) and (15) are valid for the studied parameter ranges. The divergence between the results estimated using Eq. (14) and the experimental values is presented in Fig. 10, which indicates good fitting accuracy of the proposed model, with an R^2 value of 0.863. This model is a simple equation and avoids complex differential equations, and one can determine the effect of different parameters directly from this equation.

Comparison of Proposed Model and Other Models

The proposed equation (Table 7, Column H) provides a better match with the test results (Table 7, Column A) than the previously proposed formulae. For concrete at 12 months of exposure, the mean ratio of test results to the results of the proposed equation was 0.958, with a standard deviation (SD) of 0.122. The experimental diffusion coefficient results in this study were less than those obtained using equations proposed by Samson et al. (2005) and Samson and Marchand (2007) (Table 7, Columns C and D). The mean ratio of experimental test results to the predicted values at 12 months of exposure were 2.696 and 1.194, with standard deviations of 0.874 and 0.41, respectively. The equation of Samson et al. (2003) (Table 7, Column E) gave diffusion coefficient values less than those presented in this study. The mean ratio of test results to the results of predicted equation was 1.147, with a standard deviation of 0.376. All the previous models were proposed to introduce the pore-filling effect. Samson and Marchand assumed that

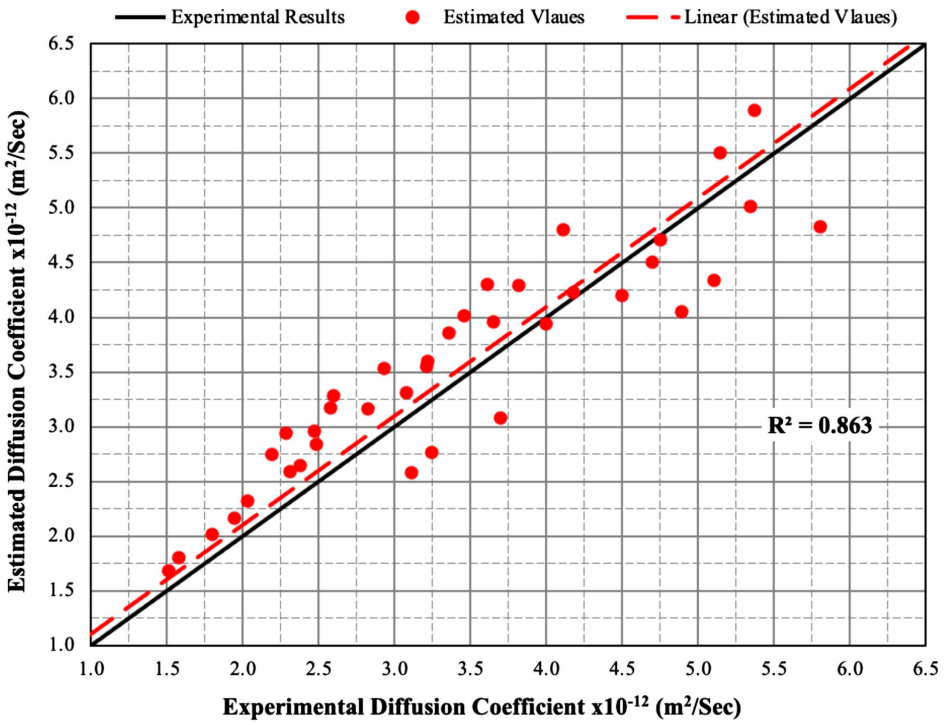

Fig. 10. Relationship between theoretical results and experimental values for sulfate ion diffusion coefficient in concrete.

Table 7. Sulfate ion diffusion coefficients calculated using different equations and experimental sulfate ions diffusion coefficients at 12 months

	Sulfate ion diffusion coefficient at 12 months age (10^{-12} m^2/s)								Diffusion coefficient experiment/prediction						
Mix ID	A	B	C	D	E	F	G	H	A/B	A/C	A/D	A/E	A/F	A/G	A/H
Control	4.00	573	1.17	2.81	2.93	—	45.8	3.94	0.007	3.42	1.42	1.37	—	0.09	1.02
FA20	2.47	573	1.17	2.81	2.93	—	45.8	2.96	0.004	2.11	0.88	0.84	—	0.05	0.84
FA40	1.95	573	1.17	2.81	2.93	—	45.8	2.16	0.003	1.66	0.69	0.66	—	0.04	0.90
FA40-1	3.22	343	1.17	2.8	2.77	0.53	45.8	3.60	0.009	2.75	1.15	1.16	6.07	0.07	0.89
FA40-2	2.19	573	1.25	2.51	2.52	0.8	57.6	2.75	0.004	1.75	0.87	0.87	2.74	0.04	0.80
FA40-3	1.51	343	1.17	2.8	2.47	0.49	45.8	1.68	0.004	1.29	0.54	0.61	3.09	0.03	0.90
FA40-4	2.38	673	1.25	2.51	3.21	0.6	16.5	2.65	0.004	1.90	0.95	0.74	—	0.14	0.90
LS20	3.46	573	1.17	2.81	2.93	—	45.8	4.02	0.006	2.96	1.23	1.18	—	0.08	0.86
LS40	3.08	573	1.17	2.81	2.93	—	45.8	3.31	0.005	2.63	1.10	1.05	—	0.07	0.93
LS40-1	5.14	343	1.17	2.8	2.77	0.53	45.8	5.50	0.015	4.40	1.84	1.86	9.70	0.11	0.93
LS40-2	4.50	573	1.25	2.51	2.52	0.8	57.6	4.20	0.008	3.60	1.79	1.79	5.63	0.08	1.07
LS40-3	3.11	343	1.17	2.8	2.47	0.49	45.8	2.58	0.009	2.66	1.11	1.26	6.35	0.07	1.21
LS40-4	4.89	673	1.25	2.51	3.21	0.6	16.5	4.05	0.007	3.91	1.95	1.52	8.15	0.30	1.21
Mean									0.007	2.696	1.194	1.147	5.960	0.090	0.958
SD									0.003	0.874	0.410	0.376	2.171	0.064	0.122

the pore-clogging (obstruction of capillary pores) does not necessarily yield a zero diffusion coefficient; they suggested that the diffusion process may occur through the gel pores (nanopores), even if they are disconnected (Samson and Marchand 2007). These relationships have good compatibility with the equation proposed in the present research in moderate-strength concrete; concretes with low and high strength have high divergence between the previous formulae and the proposed equation. The results of Oh and Jang (2004), Tu et al. (2013), and the STADIUM model (Bonakdar et al. 2012; Galíndez and Molinero 2010) (Table 7, Columns B, F, and G, respectively) had low compatibility with the results of the proposed equation. Moreover, the previous conclusion is confirmed for mixes with a content of 450 kg/m^3, which had a high difference between the experimental and predicted diffusion coefficients.

Conclusions

From the results, the following conclusions can be drawn:

1. Cement blending with any level of blending of FA and LS can decrease the initial compressive strength of concrete by 15.8% and 31.6%, respectively, compared with that of the control mix. Due to cement blending, concrete made with 20% and 40% FA had better strength loss by 23.3% and 25.6% than the control mix.
2. The sulfate ion penetration resistance of concrete noticeably improved with blended FA and LS cement binder. FA and LS blended binders had 21% and 19% lower sulfate ion penetration than pure OPC mixtures, respectively.
3. The results of sulfate ions penetration in concrete showed that binder blending helped to minimize the diffusion coefficient of

concrete with FA and LS blended binders. This reduction of diffusion coefficient was as much as 38% and 14% compared with that of the control mix, respectively.

4. The diffusion coefficient value of magnesium sulfate ions in concrete decrease by 33% and 39% as binder content increased to 400 and 450 kg/m^3, respectively. Due to the pore-filling effect, the concrete diffusion coefficient value decreased by 12% and 15% as the exposure period increased to 8 and 12 months, respectively.
5. The sulfate ion diffusion coefficient increased by 33% and 58% as water–binder ratio increased to 0.45 and 0.55, respectively.
6. A simple equation is proposed to calculate the diffusion coefficient of sulfate ions in concrete [Eq. (15)]. This model is a function of binder content, water–binder ratio, replacement ratio, and calcium-silicate content in the replacement materials.
7. The proposed model equation agreed well with other referenced models in estimating of sulfate ion diffusion coefficient, with a good mean value, about 0.958, and a low standard deviation, 0.122. It also had good correlation with Samson et al. (2003), and Samson and Marchand (2007) models.

Data Availability Statement

All data, models, and code generated or used during the study appear in the published article.

References

ACI (American Concrete Institute). 1991. *Standard practice for selecting proportions for normal, heavyweight, and mass concrete*. ACI 211.1-91. Farmington Hills, MI: ACI.

ASTM. 1996. *Standard test method for fineness of portland cement by the turbidimeter.* ASTM C115-96. West Conshohocken, PA: ASTM.

ASTM. 2005. *Standard test methods for chemical resistance of mortars, grouts, and monolithic surfacings and polymer concretes*. ASTM C267-01. West Conshohocken, PA: ASTM.

ASTM. 2007. *Standard test method for the determination of aluminum in ores and related materials by comlexometric titrimetry.* ASTM E738-11. West Conshohocken, PA: ASTM.

ASTM. 2009. *Standard specification for portland cement.* ASTM C150-07. West Conshohocken, PA: ASTM.

ASTM. 2012. *Standard specification for chemical admixtures for concrete*. ASTM C494/C494M-11. West Conshohocken, PA: ASTM.

ASTM. 2015. *Standard specification for coal fly ash and raw or calcined natural pozzolan for use in concrete*. ASTM C618-15. West Conshohocken, PA: ASTM.

Bonakdar, A., B. Mobasher, and N. Chawla. 2012. "Diffusivity and microhardness of blended cement materials exposed to external sulfate attack." *Cem. Concr. Compos.* 34 (1): 76–85. https://doi.org/10.1016/j.cemconcomp.2011.08.016.

BSI (British Standards Institution). 2009. *Testing hardened concrete. Part 1: Shape, dimensions and other requirements of specimens and moulds*. BS EN 12390-1. London: BSI.

Cai, R., T. Han, W. Liao, J. Huang, D. Li, A. Kumar, and H. Ma. 2020. "Prediction of surface chloride concentration of marine concrete using ensemble machine learning." *Cem. Concr. Res.* 136 (Oct): 106164. https://doi.org/10.1016/j.cemconres.2020.106164.

Cai, R., M. Yu, Y. Hu, L. Yang, and H. Ma. 2021. "Influence of data acquisition and processing on surface chloride concentration of marine concrete." *Constr. Build. Mater.* 273 (Mar): 121705. https://doi.org/10.1016/j.conbuildmat.2020.121705.

Chatterji, S. 1995. "On the applicability of Fick's second law to chloride ion migration through Portland cement concrete." *Cem. Concr. Res.* 25 (2): 299–303. https://doi.org/10.1016/0008-8846(95)00013-5.

Chen, Y., P. Liu, R. Zhang, Y. Hu, and Z. Yu. 2020a. "Chemical kinetic analysis of the activation energy of diffusion coefficient of sulfate ion in concrete." *Chem. Phys. Lett.* 753 (Aug): 137596. https://doi.org/10.1016/j.cplett.2020.137596.

Chen, Z., L. Wu, V. Bindiganavile, and C. Yi. 2020b. "Coupled models to describe the combined diffusion-reaction behaviour of chloride and sulphate ions in cement-based systems." *Constr. Build. Mater.* 243 (May): 118232. https://doi.org/10.1016/j.conbuildmat.2020.118232.

Chen, Z., C. Yi, and V. Bindiganavile. 2018. "Investigating the two-dimensional diffusion-reaction behaviour of sulphate ions in cement-based systems." *Constr. Build. Mater.* 187 (Oct): 791–802. https://doi.org/10.1016/j.conbuildmat.2018.07.190.

Crank, J. 1979. *The mathematics of diffusion*. Oxford, UK: Oxford University Press.

Crank, J., and R. S. Gupta. 1972. "A method for solving moving boundary problems in heat flow using cubic splines or polynomials." *IMA J. Appl. Math.* 10 (3): 296–304. https://doi.org/10.1093/imamat/10.3.296.

Diab, A. M., H. E. Elyamany, M. Abd Elmoaty, and A. H. Shalan. 2019. "Estimation of critical ettringite content due to sulfate attack." *ACI Mater. J.* 116 (6): 55–64. https://doi.org/10.14359/51716977.

Dimitriou, G., P. Savva, and M. F. Petrou. 2018. "Enhancing mechanical and durability properties of recycled aggregate concrete." *Constr. Build. Mater.* 158 (Jan): 228–235. https://doi.org/10.1016/j.conbuildmat.2017.09.137.

Galíndez, J. M., and J. Molinero. 2010. "On the relevance of electrochemical diffusion for the modeling of degradation of cementitious materials." *Cem. Concr. Compos.* 32 (May): 351–359. https://doi.org/10.1016/j.cemconcomp.2010.02.006.

Gao, D., Q. Che, Y. Meng, L. Yang, and X. Xie. 2022. "Properties evolution of calcium sulfoaluminate cement blended with ground granulated blast furnace slag suffered from sulfate attack." *J. Mater. Res. Technol.* 17 (Mar): 1642–1651. https://doi.org/10.1016/j.jmrt.2022.01.133.

Gospodinov, P., R. Kazandjiev, and M. Mironova. 1996. "The effect of sulfate ion diffusion on the structure of cement stone." *Cem. Concr. Compos.* 18 (6): 401–407. https://doi.org/10.1016/S0958-9465(96)00032-7.

Gospodinov, P. N., R. F. Kazandjiev, T. A. Partalin, and M. K. Mironova. 1999. "Diffusion of sulfate ions into cement stone regarding simultaneous chemical reactions and resulting effects." *Cem. Concr. Res.* 29 (10): 1591–1596. https://doi.org/10.1016/S0008-8846(99)00138-6.

Hefni, Y., Y. Abd El Zaher, and M. A. Wahab. 2018. "Influence of activation of fly ash on the mechanical properties of concrete." *Constr. Build. Mater.* 172 (May): 728–734. https://doi.org/10.1016/j.conbuildmat.2018.04.021.

Huang, Q., G. Xiong, Z. Fang, S. Wang, C. Wang, H. Sun, S. Yuan, and X. Zhu. 2023. "Long-term performance and microstructural characteristics of cement mortars containing nano-SiO_2 exposed to sodium sulfate attack." *Constr. Build. Mater.* 364 (Jan): 130011. https://doi.org/10.1016/j.conbuildmat.2022.130011.

Jin, L., Z. Wang, B. Yang, T. Wu, Q. Wu, and P. Zhou. 2024. "Mesoscopic numerical simulation of sulfate ion transport behavior in concrete based on a new damage model." *Structures* 61 (Mar): 106066. https://doi.org/10.1016/j.istruc.2024.106066.

Kou, S.-C., C.-S. Poon, and F. Agrela. 2011. "Comparisons of natural and recycled aggregate concretes prepared with the addition of different mineral admixtures." *Cem. Concr. Compos.* 33 (8): 788–795. https://doi.org/10.1016/j.cemconcomp.2011.05.009.

Kurad, R., J. D. Silvestre, J. de Brito, and H. Ahmed. 2017. "Effect of incorporation of high volume of recycled concrete aggregates and fly ash on the strength and global warming potential of concrete." *J. Cleaner Prod.* 166 (Nov): 485–502. https://doi.org/10.1016/j.jclepro.2017.07.236.

Li, C., J. Li, Q. Ren, Y. Zhao, and Z. Jiang. 2022. "Degradation mechanism of blended cement pastes in sulfate-bearing environments under applied electric fields: Sulfate attack vs. decalcification." *Composites, Part B* 246 (Nov): 110255. https://doi.org/10.1016/j.compositesb.2022.110255.

Li, K., T. Wu, A. P. S. Arunachalam, L. Zhao, and Q. Liu. 2023. "A diffusion-reaction model for sulfate ion corrosion in multi-phase concrete immersed in ionic solution." *Ceram. Int.* 49 (9): 14064–14078. https://doi.org/10.1016/j.ceramint.2022.12.288.

Liu, Z., Y. Zhang, and Q. Jiang. 2014. "Continuous tracking of the relationship between resistivity and pore structure of cement pastes." *Constr. Build. Mater.* 53 (Feb): 26–31. https://doi.org/10.1016/j.conbuildmat.2013.11.067.

Locoge, P., M. Massat, J. P. Ollivier, and C. Richet. 1992. "Ion diffusion in microcracked concrete." *Cem. Concr. Res.* 22 (2–3): 431–438. https://doi.org/10.1016/0008-8846(92)90085-A.

Marchand, J., E. Samson, and Y. Maltais. 1999. "Modeling microstructural alterations of concrete subjected to external sulfate attack." In *Materials science of concrete: Sulfate attack mechanisms(USA)*, 211–257. Columbus, OH: American Ceramic Society.

Masood, B., A. Elahi, S. Barbhuiya, and B. Ali. 2020. "Mechanical and durability performance of recycled aggregate concrete incorporating low calcium bentonite." *Constr. Build. Mater.* 237 (Mar): 117760. https://doi.org/10.1016/j.conbuildmat.2019.117760.

Medeiros, M. H. F., and P. R. D. L. Helene. 2009. "Surface treatment of reinforced concrete in marine environment: Influence on chloride diffusion coefficient and capillary water absorption." *Constr. Build. Mater.* 23 (3): 1476–1484. https://doi.org/10.1016/j.conbuildmat.2008.06.013.

Oh, B. H., and S. Y. Jang. 2004. "Prediction of diffusivity of concrete based on simple analytic equations." *Cem. Concr. Res.* 34 (3): 463–480. https://doi.org/10.1016/j.cemconres.2003.08.026.

Provis, J. L., and J. S. J. van Deventer. 2009. *Geopolymers: Structures, processing, properties and industrial applications*. Amsterdam, Netherlands: Elsevier.

Qian, J., C. Shi, and Z. Wang. 2001. "Activation of blended cements containing fly ash." *Cem. Concr. Res.* 31 (8): 1121–1127. https://doi.org/10.1016/S0008-8846(01)00526-9.

Samson, E., and J. Marchand. 2007. "Modeling the transport of ions in unsaturated cement-based materials." *Comput. Struct.* 85 (23–24): 1740–1756. https://doi.org/10.1016/j.compstruc.2007.04.008.

Samson, E., J. Marchand, and K. A. Snyder. 2003. "Calculation of ionic diffusion coefficients on the basis of migration test results." *Mater. Struct.* 36 (Apr): 156–165. https://doi.org/10.1007/BF02479554.

Samson, E., J. Marchand, K. A. Snyder, and J. J. Beaudoin. 2005. "Modeling ion and fluid transport in unsaturated cement systems in isothermal conditions." *Cem. Concr. Res.* 35 (1): 141–153. https://doi.org/10.1016/j.cemconres.2004.07.016.

Shafikhani, M., and S. E. Chidiac. 2020. "A holistic model for cement paste and concrete chloride diffusion coefficient." *Cem. Concr. Res.* 133 (Jul): 106049. https://doi.org/10.1016/j.cemconres.2020.106049.

Shalan, A. H., and M. El-Gohary. 2022. "Long-term sulfate resistance of blended cement concrete with waste glass powder." *Pract. Period. Struct. Des. Constr.* 27 (4): 04022047. https://doi.org/10.1061/(ASCE)SC.1943-5576.0000731.

Tixier, R. 2000. *Microstructural development and sulfate attack modeling in blended cement-based materials*. Tempe, AZ: Arizona State Univ.

Tixier, R., and B. Mobasher. 2003a. "Modeling of damage in cement-based materials subjected to external sulfate attack. I: Formulation." *J. Mater. Civ. Eng.* 15 (4): 305–313. https://doi.org/10.1061/(ASCE)0899-1561(2003)15:4(305).

Tixier, R., and B. Mobasher. 2003b. "Modeling of damage in cement-based materials subjected to external sulfate attack. II: Comparison with experiments." *J. Mater. Civ. Eng.* 15 (4): 314–322. https://doi.org/10.1061/(ASCE)0899-1561(2003)15:4(314).

Tu, W., G. S. Cunningham, Y. Chen, M. G. Henderson, E. Camporeale, and G. D. Reeves. 2013. "Modeling radiation belt electron dynamics during GEM challenge intervals with the DREAM3D diffusion model." *J. Geophys. Res.: Space Phys.* 118 (10): 6197–6211. https://doi.org/10.1002/jgra.50560.

Velandia, D. F., C. J. Lynsdale, J. L. Provis, and F. Ramirez. 2018. "Effect of mix design inputs, curing and compressive strength on the durability of Na_2SO_4-activated high volume fly ash concretes." *Cem. Concr. Compos.* 91 (Aug): 11–20. https://doi.org/10.1016/j.cemconcomp.2018.03.028.

Velandia, D. F., C. J. Lynsdale, J. L. Provis, F. Ramirez, and A. C. Gomez. 2016. "Evaluation of activated high volume fly ash systems using Na_2SO_4, lime and quicklime in mortars with high loss on ignition fly ashes." *Constr. Build. Mater.* 128 (Dec): 248–255. https://doi.org/10.1016/j.conbuildmat.2016.10.076.

Wang, G., Q. Wu, H. Zhou, C. Peng, and W. Chen. 2021. "Diffusion of chloride ion in coral aggregate seawater concrete under marine environment." *Constr. Build. Mater.* 284 (May): 122821. https://doi.org/10.1016/j.conbuildmat.2021.122821.

Wang, H.-L., J.-J. Wang, X.-Y. Sun, and W.-L. Jin. 2013. "Improving performance of recycled aggregate concrete with superfine pozzolanic powders." *J. Cent. South Univ.* 20 (12): 3715–3722. https://doi.org/10.1007/s11771-013-1899-7.

Wu, T., L. Jin, T. Fan, L. Qiao, P. Liu, P. Zhou, and Y. Zhang. 2023. "A multi-phase numerical simulation method for the changing process of expansion products on concrete under sulfate attack." *Case Stud. Constr. Mater.* 19 (Dec): e02458. https://doi.org/10.1016/j.cscm.2023.e02458.

Zhang, J., J. Zhao, Y. Zhang, Y. Gao, and Y. Zheng. 2018. "Instantaneous chloride diffusion coefficient and its time dependency of concrete exposed to a marine tidal environment." *Constr. Build. Mater.* 167 (Apr): 225–234. https://doi.org/10.1016/j.conbuildmat.2018.01.107.

Zunino, F., and K. Scrivener. 2019. "The influence of the filler effect on the sulfate requirement of blended cements." *Cem. Concr. Res.* 126 (Dec): 105918. https://doi.org/10.1016/j.cemconres.2019.105918.

Zunino, F., and K. Scrivener. 2022. "Insights on the role of alumina content and the filler effect on the sulfate requirement of PC and blended cements." *Cem. Concr. Res.* 160 (Oct): 106929. https://doi.org/10.1016/j.cemconres.2022.106929.